Check for updates

Risk and life cycle assessment of nanoparticles for medical applications prepared using safe- and benign-by-design gas-phase syntheses†

P. Weyell,[a] H.-D. Kurland,[b] T. Hülser,[c] J. Grabow,[b] F. A. Müller[b] and D. Kralisch [ID] *[a]

Laser vaporisation is a promising technology for the industrial manufacturing of spherical, oxidic nanoparticles, including crystalline, less-agglomerated ferromagnetic maghemite (γ-Fe$_2$O$_3$) and superparamagnetic γ-Fe$_2$O$_3$/amorphous SiO$_2$ composite nanoparticles. These can be utilised in medical applications such as contrast agents in magnetic resonance imaging (MRI) and may replace common contrast agents such as gadolinium chelate complexes. Nano-specific risk assessment and life cycle assessment have been used in parallel in order to critically assess benefits and shortcomings of this technological approach and to find the key parameters for process optimisation. Potential risks in occupational safety were found to be low, but the energy demand of the laser system is crucial in terms of environmental impact potential. However, process optimisation options in process efficiency, laser source and reuse of waste heat were identified, leading to a decrease of the overall cumulated energy demand up to 94%. Flame spray pyrolysis was included in the comparative study as an alternative approach for gas phase synthesis of oxidic nanoparticles. Both technologies and the resulting nanoenabled products were found to be environmentally beneficial compared to the preparation of the standard MRI contrast agent Gadovist®.

Introduction

Nanotechnology is considered to be one of the six key enabling technologies having an important impact on the growth of the European process industry and well-being of the society.[1] During the last few decades, numerous synthesis procedures have been developed in order to produce nanomaterials made from different raw materials and compositions, in different sizes, forms, *etc*.[2] In some cases, the production of these nanomaterials has already overcome its infancies and reached the ton scale (*e.g.* silicon dioxide nanoparticles 599 000 t a^{-1} and iron oxide nanoparticles 9260 t a^{-1}).[3] As a result of the increasing commercial accessibility, nanoenabled products are already in use in several fields of application, including in chemistry,[4] construction,[5] pharmacy and medicine.[6]

The growing industrial demand for nanoenabled products[7] and the development of large-scale production processes[8] over the last couple of years have led to increasing safety requirements for production processes and the resulting products alike.[9] Besides that, environmental impacts of products and production processes are seen more critically, today, and are taken into consideration more often. European policies call for significant reductions in energy demand and non-renewable material consumption for all new technologies compared to the state of the art.[10] Failing these requirements may result in consequences ranging from exclusion from public funding, additional taxes to prohibitions of production.

In order to meet the ever-growing data requirements for new nanomaterials and their production processes, a consideration of *e.g.* safety aspects, environmental impacts, and resource consumption right from the beginning in research and development is highly recommended.[1,11] The additional information provided during the decision-making process for the selection of certain options at an early stage will foster the design of safer and more environmentally benign processes and products later on.[12] The clear benefits and viability of such a holistic concept, utilising *e.g.* Life Cycle Assessment (LCA) and Risk Assessment (RA), have been already approved in many case studies, *e.g.* by Kralisch *et al.*[13] and Hou *et al.*[14] However, only a few have focussed on nanotechnology, yet.[15]

[a]*Friedrich Schiller University Jena, Pharmaceutical Technology and Biopharmacy, Lessingstraße 8, 07743 Jena, Germany. E-mail: dana.kralisch@uni-jena.de; Fax: +49 3641 949942; Tel: +49 3641 949951*
[b]*Friedrich Schiller University Jena, Otto Schott Institute of Materials Research (OSIM), Löbdergraben 32, 07743 Jena, Germany*
[c]*Institut für Energie- und Umwelttechnik e.V. (IUTA), Bliersheimer Straße 58-60, 47229 Duisburg, Germany*
†Electronic supplementary information (ESI) available. See DOI: 10.1039/c9gc02436k

In this article, an early stage comparative LCA and nanomaterial specific RA study of oxidic nanoparticles, produced using laser vaporisation (LAVA) of a single metal oxide powder and by co-vaporisation (CoLAVA) of homogeneous mixtures of metal oxide powders, is presented. These laser-induced production processes for oxidic nanoparticles[16] were assessed for three reasons. First of all, the (Co)LAVA technologies are well suited for the continuous and reproducible production of high quality nanopowders with merely softly agglomerated, spherical nanoparticles of defined crystal phase(s) and narrow diameter distribution. This improvement in quality opens up new application potential, *e.g.* in the fields of medical diagnostics and therapy. Secondly, technology readiness of this promising technology has already been approved on the semi-industrial scale,[17] which is an important premise for the development of broadly applicable products. Last but not least, the CoLAVA technique allows the direct, single-stage synthesis of inorganic core–shell nanoparticles. Core–shell structures can reduce toxicological risks of the core and improve biocompatibility and colloidal stability of particles.[18]

LAVA and CoLAVA prepared magnetic iron oxide nanoparticles (IONs) with organic and inorganic shells, respectively, were selected as case studies, due to their high application potential in nanomedicine, *e.g.* as T_2 contrast agents in magnetic resonance imaging (MRI), and in theranostic and hyperthermia treatment.[19] Physicochemical properties, occupational risks, potential environmental impacts and benefits of these nanoparticles in relation to their future value in MRI diagnostics were investigated in this comparative analysis.

The results were critically compared with those for an established gadolinium-based contrast agent, taken as the baseline, and with IONs synthesized using flame spray pyrolysis (FSP), considered as a technological alternative for large-scale gasphase synthesis of metal and metal oxide nanoparticles.[20] While gadolinium chelate complexes are known for their potential nephrotoxicity,[21] are suspected to cause accumulation of gadolinium in the brain[22] and may be afflicted by comparatively high environmental impacts caused by their complex multi-step synthesis pathways, little is known about the safety and environmental impacts of gas phase nanoparticle generation procedures such as LAVA, CoLAVA or FSP.

By means of this study we are providing a profound basis for safe and environmentally benign design of a new generation of medical nanoproducts and their production processes.

Materials & methods

Synthesis of magnetic nanopowders and their physicochemical characterisation

Preparation of metal oxide nanoparticles by laser vaporisation. The (Co)LAVA methods were previously described in detail elsewhere.[16] Briefly, these methods use a CO_2 laser beam which is focused onto the surface of coarse ceramic starting powders. The LAVA process starts from a single ceramic raw powder, while the starting materials of the CoLAVA process are defined, homogeneous mixtures of ceramic raw powders. Due to absorption of the intense laser radiation, the raw powder heats up and vaporises. Further absorption processes in the vapor result in its superheating and the formation of plasma just above the beam focus. Vaporisation and plasma formation occur under normal pressure in a continuously flowing process gas. Plasma and vapour cool down rapidly when they expand into the process gas, and nanoparticles grow by an accordingly fast gas-phase condensation. Depending on the composition of the raw powder mixture CoLAVA yields mixed oxide or composite nanoparticles due to the simultaneous condensation of the components from the raw powder mixture. The nanoparticle laden gas flow (nanoparticle aerosol) transports the nanoparticles into a filter unit, where the nanopowder is finally separated.

Superparamagnetic silica coated iron oxide (SiliFe) composite nanoparticles consisting of a closed spherical matrix of amorphous silica with a maghemite (γ-Fe_2O_3) inclusion (core) (Fig. 1) were prepared by using the CoLAVA method.[23] For the synthesis, 70 mass% hematite powder (α-Fe_2O_3; Sigma-Aldrich Chemie GmbH, Steinheim, Germany, product no. 310050, purity $\geq$99%, grain size $\leq$5 μm) and 30 mass% silica powder (SiO_2; Sigma-Aldrich Chemie GmbH, Steinheim, Germany, product no. 83340, purum p.a., grain size <63 μm) were mixed in a tumbling mixer. The homogeneous mixture was vaporised with continuous CO_2 laser radiation (wavelength 10.59 μm, radiation power 2 kW, focus intensity 220 kW cm^{-2}). A total process gas flow of 14.5 m^3 h^{-1} was applied consisting of air as a background flow (12.5 m^3 h^{-1}) and argon as an additional gas flow (2 m^3 h^{-1}) directly fed into the zone of condensation. Argon was used as an additional gas since it promotes the formation of maghemite.[24,25] CoLAVA synthesis and formation of these SiliFe nanoparticles were described in detail previously.[23]

The ferromagnetic maghemite nanoparticles in this study were prepared by using the LAVA method starting from the same hematite raw powder and applying the same process conditions already used for the synthesis of the SiliFe nano-
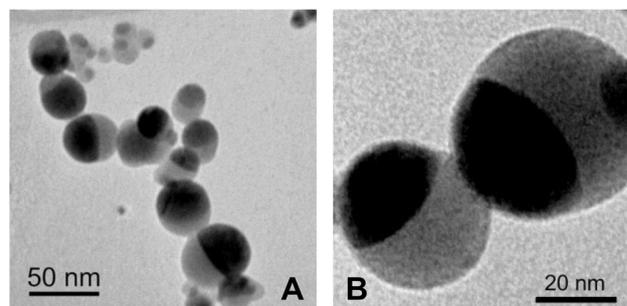

Fig. 1 TEM micrographs of SiliFe nanoparticles: amorphous silica matrix bright, maghemite inclusions dark. (A) Particle size distribution. (B) Depiction of the closed silica shell.

particles. LAVA synthesis and formation of the maghemite nanoparticles were described in detail previously.[24]

Physicochemical characterisation of the magnetic nanopowders. The nanopowders were characterised according to the technical specification document ISO/TS 17200. Morphological and structural properties of the nanoparticles were examined by transmission electron microscopy (TEM, JEM 3010, JEOL, accelerating voltage U = 300 kV). TEM micrographs were used to evaluate the size distribution of the nanoparticles by measuring and classifying the Feret diameters of about 1000 nanoparticles. From these data, the frequency distribution q_0 of the particle diameters was compiled and fitted with a logarithmic normal distribution to obtain the geometric mean particle diameter $\mu_g(q_0)$. The cumulative particle size distribution Q_0 was fitted with a sigmoid function to compile the characteristic median particle diameters d_{10}, d_{50}, and d_{90}. The frequency-based size distribution of the iron oxide inclusions in the SiliFe nanoparticles was evaluated by measuring and classifying the maximum size of about 1000 inclusions. Again the distribution was fitted with a logarithmic normal distribution to obtain the geometric mean size $\mu_{g,Inc}(q_0)$ of the iron oxide inclusions. The Brunauer–Emmett–Teller (BET) method was applied to measure the mass-specific surface area S_{BET} of a degassed nanopowder sample via nitrogen adsorption. In order to identify the crystal phases in the SiliFe nanopowder X-ray powder diffraction (XRD) measurements were conducted. The powder diffraction file PDF 39-1346 for γ-Fe$_2$O$_3$ from the Inorganic Crystal Structure Database (ICSD) was used as a reference. The mean crystallite size $L_{(311)}$ of the iron oxide inclusions was calculated by using the Scherrer equation (eqn (1)) from the full width at half-maximum $\Delta_{(311)}$ of the (311) reflection of γ-Fe$_2$O$_3$, its diffraction angle 2θ, the wavelength λ of the X-ray radiation, and the Scherrer constant K assuming a spherical geometry (K = 0.89). The value of $\Delta_{(311)}$ was corrected for the instrumental broadening Δ_i determined from the XRD measurement of a LaB$_6$ standard.

$$L_{(hkl)} = \frac{K \cdot \lambda}{\cos 2\theta \cdot \sqrt{\Delta_{(hkl)}^2 - \Delta_i^2}} \qquad (1)$$

Vibrating sample magnetometry was applied to measure the saturation and remanent magnetisation M_S and M_R, respectively, of the composite nanopowder.

Elemental impurities

The elemental composition was determined by XRF spectroscopy (S8 Tiger spectrometer from Bruker) in a non-destructive testing. Elemental concentrations in the ppm range were assessed by semi-quantitative analysis using the device specific software SpectraPlus. Since contrast agents have to fulfil the requirements for parenterals, the compliance of the chemical composition of the nanopowders with requirements concerning elemental impurities in pharmaceuticals (ICH-Q3D)[26] was investigated applying X-ray fluorescence (XRF) spectroscopy. The impurities observed in XRF spectroscopy (ESI, Table 1†) were analysed in relation to the element-specific permitted

daily exposures (PDE) per applied dose. The PDE expresses limits for residues of, e.g. metal catalysts and metal reagents in pharmaceutical products and exposure of permissible masses per day.

Life cycle assessment

LCA and RA were used in this study to evaluate and support safe- and environmentally benign-by-design process and material development.

LCA is a compilation and evaluation of the inputs, outputs and potential environmental impacts of a product throughout its entire life cycle (from cradle to grave).[27] In accordance with ISO 14040/44, LCA comprises four stages: (1) goal and scope definition, (2) life cycle inventory analysis, (3) life cycle impact assessment (LCIA) and (4) interpretation of results. The goal and scope definition is the most crucial step in an LCA study due to the necessary description of the exact utility of the product and the product system including assumptions, allocations and system boundaries. The life cycle inventory (LCI) comprises quantified input and output data (mass and energy data) along the life cycle of the product system under study, starting with raw material extraction, production and manufacturing, application up to waste treatment and/or recycling. During the LCIA, the potential environmental impacts are calculated based on the LCI data. Before doing so, relevant environmental categories as well as indicators and related methods for the characterisation model have to be identified.

In this study, IPCC2013[28] was chosen for the assessment of the global warming potential (GWP) and CML[29] as established and the robust LCIA method for the assessment of further life cycle impacts as summarised in Table 1. Since contrast agents are medical or pharmaceutical products, human and ecotoxicity have a particularly high relevance in this specific study. USEtox, recommended as the most established LCIA method for the LCIA of potential toxicological impacts of pharmaceuticals,[30] was used in this study to assess the human (HTP) and ecotoxicity potential (ETP).

Goal and scope definition. A comparative LCA study on magnetic iron oxide nanoparticles (SiliFe and γ-Fe$_2$O$_3$ nanoparticles with an organic shell) generated by (Co)LAVA technology through gas phase synthesis and their applicability as T_2 contrast agents in MRI exams was performed (Fig. 2). IONs

Table 1 Impact categories and indicators in LCIA

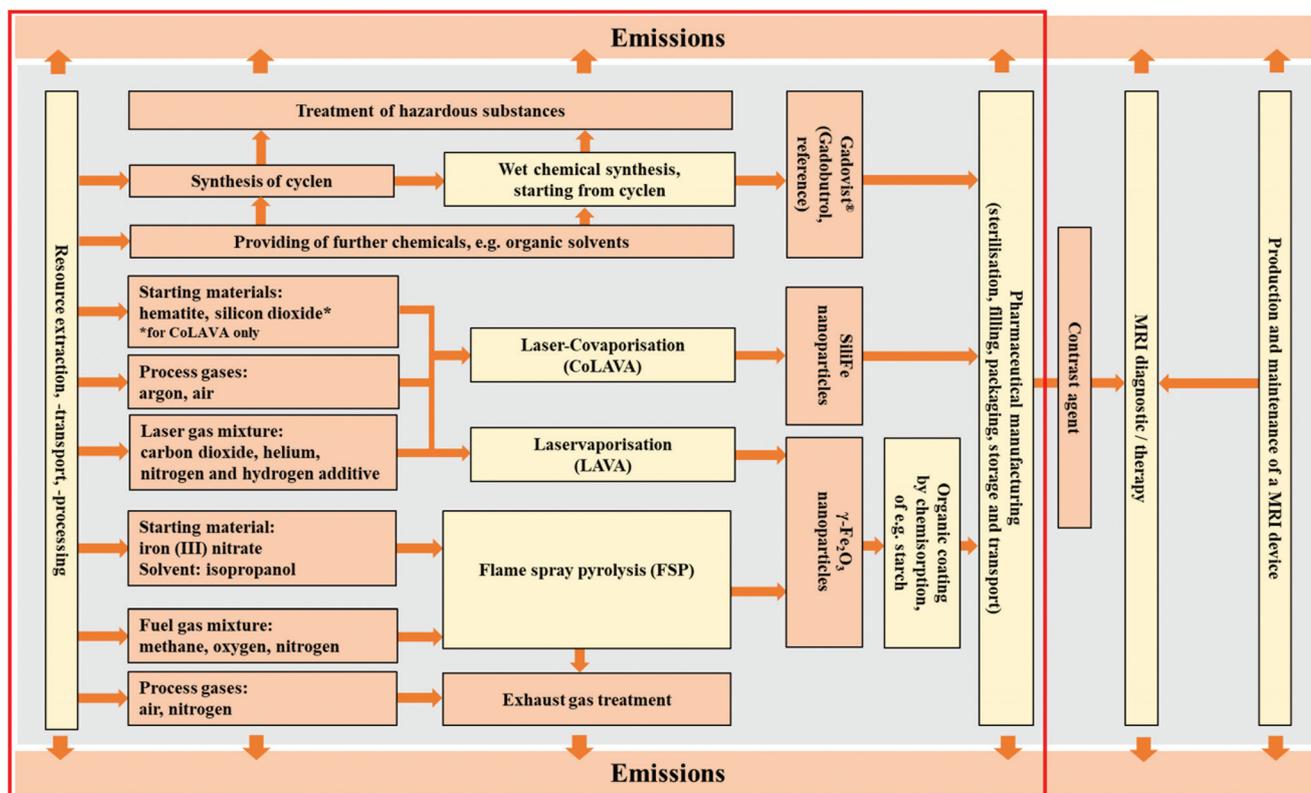| Method	Impact category	Indicator
IPCC 2013	Climate change	GWP
CML 2001	Acidification	AP
	Eutrophication	EP
	Photochemical oxidation	POCP
	Ozone depletion	ODP
	Abiotic resource depletion	
	Metals & minerals	ADP$_{elemental}$
	Fossil fuels	ADP$_{fossil}$
USEtox	Human toxicity	HTP
	Aquatic ecotoxicity	ETP

Fig. 2 System boundary for life cycle assessment. Comparative approach in the evaluation of γ-Fe$_2$O$_3$ and SiliFe nanoparticles; reference process gadolinium chelate complex Gadovist® production.

without an inorganic or organic shell possess a certain risk to induce the formation of radical oxygen species (ROS) by the Fenton and Haber–Weiss reactions.[31] Consequently, only core–shell IONs were analysed in this study. Alternative scenarios of processing were investigated in order to quantify the current environmental impact potential and to point out the key parameters for improvements.

The wet chemical synthesis of the gadolinium chelate complex (GCC) Gadovist® as a common contrast agent without a nanoenabled functionality was analysed as the baseline (Fig. 2).

Furthermore, FSP was considered as an alternative established gas phase synthesis process of oxide nanoparticles. The TEM image of iron oxide nanoparticles generated in a flame spray process on a pilot plant scale is depicted in ESI, Fig. 1.† In the case of FSP, kinetically controlled particle formation occurs by the combustion of liquid precursor materials, which are often mixed or diluted with fuels (alcohol solvents) but do not require an additional source of energy for precursor conversion. FSP readily utilises less-volatile and economical precursors such as metal acetates or nitrates and allows the generation of functional nanocomposites, *e.g.* core–shell structures.[20]

The data for modelling of both (Co)LAVA and FSP were collected from two pilot-scale plants installed at Friedrich Schiller University Jena (FSU) (Fig. 3) and the Institute for Energy and Environmental Technology (IUTA) (Fig. 4) as well as from the literature.[32–36] The manufacturing process for the LCA reference product Gadovist® was modelled based on the literature data,[37] since no detailed LCI information about the current production process could be obtained.

After the manufacturing of the GCC or nanoparticles, further steps are required in order to obtain the final product, *e.g.* dispersion of the nanoparticles and filling of the injectable suspension, packaging of the contrast agent and transport of the final pharmaceutical product. These down-stream process steps were included in the cradle-to-gate evaluation of all scenarios alike by consideration of the generic data obtained from the environmental declaration of TEVA Pharmaceutical Industries (ESI, Table 2†).[38]

In case secondary data were needed for comparative evaluation, the software Umberto NXT LCA 7.1.13 and the database ecoinvent version 2.2 and 3.2 were used for LCI modelling. Further information was obtained through expert interviews or from the scientific literature.

Detailed information about the datasets used in the LCI and a data quality rating are provided in ESI, Tables 3 and 4.†

Functional unit. The definition of functional unit (FU) allows the relation of potential environmental impacts of a product on its function rather than its physical properties. By that, products made from different materials but featuring the same functionality become comparable.
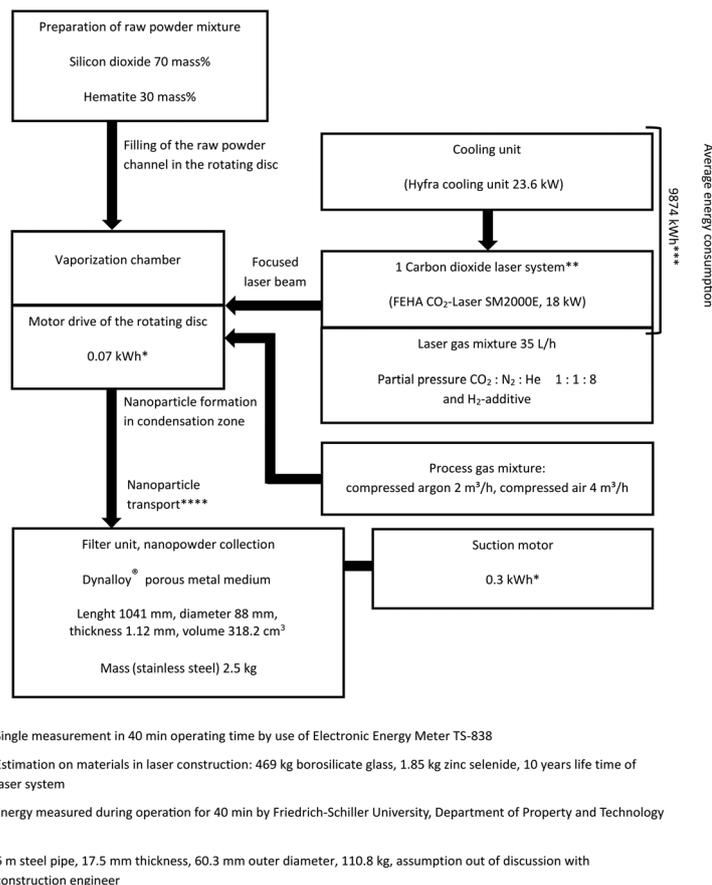
Fig. 3 Primary and secondary (literature[32–34]) data of the CoLAVA process.

Iron oxide (composite) nanoparticles produced by CoLAVA, LAVA and FSP were compared with Gadovist® based on their applicability as contrast agents in MRI exams. In the case of nanoenabled products, a unit dose for a patient with 70 kg body weight (bw) was considered in all calculations. This FU was determined based on mass doses of the former contrast agents Feridex® (15 μmol Fe per kg body weight) and Resovist® (10 μmol Fe per kg body weight) (Table 2). Values were calculated based on XRF analysis of the chemical composition of the nanoparticles (ESI, Table 1†). The FU for the reference Gadovist® was determined on the basis of the recommended single injection dose of 7 mL (4.2 g gadobutrol, 0.1 mmol Gd per kg body weight) before MRI exams.

Scenarios. Different scenarios were evaluated in order to critically assess and compare the potential environmental impacts resulting from alternative measures to obtain the same functional unit and to point out possible improvements of the existing nanoparticle generation processes.

The synthesis of the GCC Gadovist® as a contrast agent in MRI and the resulting environmental impact potential were assessed in Scenario 1 (baseline):

Gadovist S1: Wet chemical synthesis of Gadovist®. The LCI data were collected based on a typical chemical synthesis pathway for the gadolinium complex (Fig. 5). The upstream processes in the preparation of the butrol ligand (1), and complexation of gadobutrol (2) by addition of gadolinium oxide Gd_2O_3 as an active ingredient and the down-stream processes (e.g. packaging and waste treatment) were integrated in the evaluation as well. Information about the database and the assumptions made for modelling are summarised in ESI, Table 5.†

Scenarios 2–5 comprise the current CoLAVA technology and different options for process parameter variations. The LCI of the CoLAVA process for SiliFe nanoparticle generation was evaluated based on the primary data of the pilot-scale system (Fig. 3). The apparatus consists of three laser systems used in parallel. A maximum production rate of 3×60 g h^{-1} nanoparticles can be achieved in this setup.

CoLAVA S2: Production of SiliFe nanoparticles in a CoLAVA plant with three carbon dioxide laser systems and a production rate of 180 g h^{-1} installed in a future industrial environment.

Alternatives to improve the environmental impact by optimisation of the plant setup were analysed in Scenarios CoLAVA 3–5 based on recent findings described in the literature. An installation of a heating pump and reuse of the released waste heat of the laser cooling unit could reduce the overall process energy consumption up to 45%.[39] New technical developments such as fiber and disk laser systems could
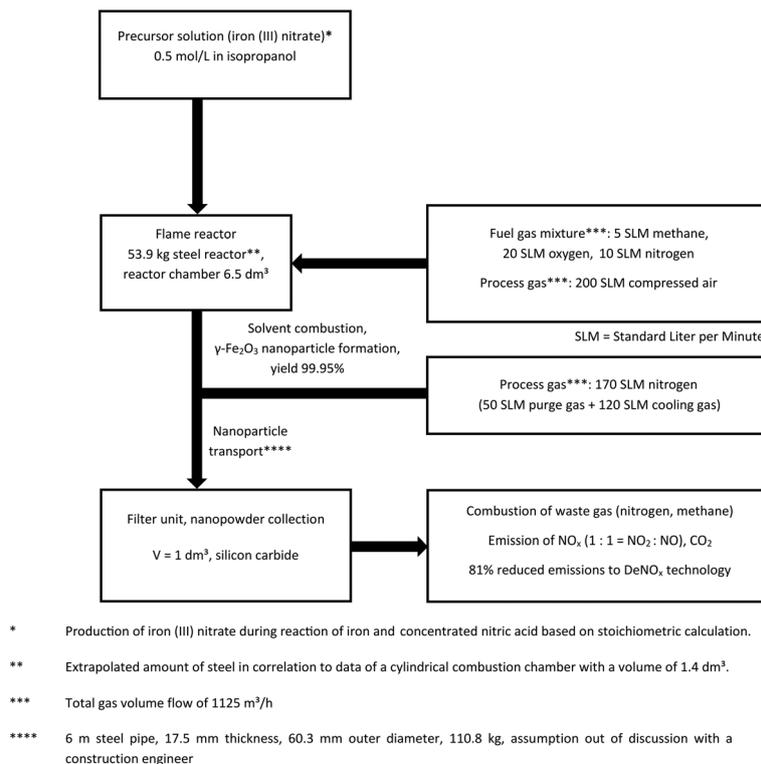
Fig. 4 Primary and secondary (literature[35,36]) data of flame spray pyrolysis (FSP).

Table 2 Mass doses of nanoparticles and Gadovist® for a 70 kg person as a functional unit (FU) in LCA (bw = body weight)

		FU in LCA mass dose [mg]	
Process technology	Contrast agent	15 μmol Fe per kg bw	10 μmol Fe per kg bw
CoLAVA	SiliFe	231	154
LAVA	γ-Fe_2O_3	84	56
FSP	γ-Fe_2O_3	84	56
Wet chemical synthesis	Gadovist®	4200	

further reduce the energy consumption up to 50% compared to conventional carbon dioxide lasers.[40]

CoLAVA S3: CoLAVA S2, but with an additional installation of a heat pump for the laser cooling unit and waste heat utilisation.

CoLAVA S4: Reduction of the energy demand of the laser system (based on S2) by exchange of the laser beam source(s).

CoLAVA S5: Optimisation of the CoLAVA process setup and exchange of the laser beam source(s) (combination of S3 and S4).

The production of γ-Fe_2O_3 instead of SiliFe nanoparticles was assessed in Scenarios LAVA S6 and S7. Process conditions were assumed to be the same as in the CoLAVA 2 or 5 scenarios except for the use of hematite as a single raw material. Since γ-Fe_2O_3 nanoparticles without a silica coating would have a high risk of ROS formation after injection as a contrast agent,

post-modification by chemisorption of starch as a typical organic coating was assumed in LCI modelling, based on a study by Schlenk *et al.*[41] The group could show that the toxicity of iron oxide nanoparticles can be significantly reduced by neutral or anionic polymer coatings.

LAVA S6: Synthesis of γ-Fe_2O_3 nanoparticles by LAVA technology (process setup based on S2) – a *post*-process nanoparticle coating with starch.

LAVA S7: Combination of optimisation measures (based on CoLAVA S5) for the synthesis of γ-Fe_2O_3 nanoparticles coated with starch.

FSP S8: FSP for the generation of γ-Fe_2O_3 nanoparticles, the precursor solution iron(III) nitrate in 0.5 mol L^{-1} isopropanol, a production rate of 270 g h^{-1} and *post*-process modification of the nanoparticles by chemisorption of starch.

Occupational safety analysis

The LCA approach is generally applicable for the evaluation of potential environmental impacts of nanotechnology, but missing nano-specific characterisation models in LCIA (*e.g.* due to size dependent altered properties and varying behaviour in contrast to bulk chemicals) limit the significance of the results.[42] Here, human health and/or environmental RA can be used in a complementary way[27] to close current nano-specific gaps in nanoparticle production processes using Stoffenmanager Nano.[43]

By the definition of the World Health Organization (WHO),[44] HHRA allows the identification of a substance
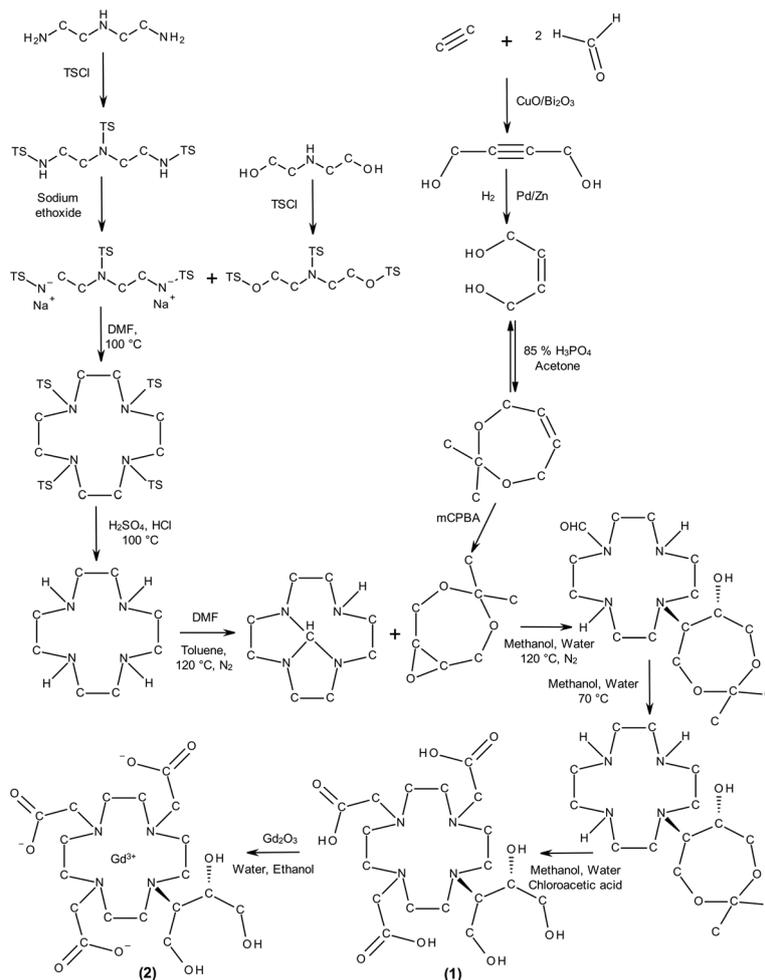
Fig. 5 Synthesis of gadobutrol (Gadovist®). (TS = tosyl, TSCl = tosyl chloride, DMF = *N,N*-dimethylformamide, *m*CPBA = *meta*-chloroperoxybenzoic acid).

causing harm to people (hazard characterisation) and quantification of the exposition (exposure assessment) in a specific scenario (problem formulation).[27] The resulting risks are assessed by numerical relationships between exposure and effects as well as frequency, time and levels of contact with a certain stressor. The opportunities to control, reduce or avoid the risks identified are then evaluated for risk management.

In our case, hazard characterisation was based on the toxicological data obtained from the literature. Since it is yet unknown whether the potential new contrast agent will be registered as a medical or pharmaceutical product, both ISO 10993 and ICH guidance documents[45] were taken into account during the evaluation.

The analysis of potential occupational safety issues was performed considering additional life cycle steps of a theoretical future production process. State of the art technologies, which would be used in a scaled-up (Co)LAVA process or FSP, were identified by a literature review, *e.g.* for raw material transport during technical processing,[46] *post*-process modification by organic coating, separation, dispersion, purification and steri-

lisation of the nanoparticles.[47] The results were summarised in process schemes to identify potential risks and challenges in ensuring occupational safety.

Nano-specific risks were identified by the control banding approach applied in compliance with ISO/TG 12901-2 using Stoffenmanager Nano[43] and the online tool (https://nano.stoffenmanager.nl/). Scenarios A–D were defined in order to identify potential future nano-specific risks occurring during the production phase of the nanoenabled products (Table 3).

In hazard characterisation of SiliFe and γ-Fe$_2$O$_3$ nanoparticles, the literature data were used. A previous study by Stötzel *et al.*[23] showed that SiliFe nanoparticles have a similar surface behavior to that of pure silica nanoparticles indicating a closed silica shell (matrix) around the γ-Fe$_2$O$_3$ inclusion (core). Thus, the hazard data provided in a safety data sheet of silica nanoparticles[48] as an analogous material could be used (in compliance with ISO/TG 12901-2). The data considered in categories such as acute toxicity, irritation, cancerogenity, mutagenicity and reproductive toxicity are summarised in ESI, Table 6†. γ-Fe$_2$O$_3$ nanoparticles coated with starch were ana-

Table 3 Scenarios in nano-specific occupational risk assessment

Scenario	Risk analysis in:
A	Continuous manufacturing of nanoparticles in an enclosed (Co)LAVA process or FSP. Process control by employees in a separate control room
B	Maintenance of the process plant (*e.g.* exchange of the filter system) once a year without/with the use of personal protective equipment (filter mask FPP2 or full-face powered air respirator TMP3)
C	Filling and packaging of the nanoparticles as a sterile pharmaceutical product; change in exposure risk due to the separate filling system (*e.g.* a glove box)
D	Transport and storage of the packaged end product

lysed based on screening toxicity data on core–shell iron oxide nanoparticles published by Schlenk *et al.*[41] The study included physicochemical characterisation, stability in biological media over 28 days, *in vitro* cytotoxicity, *in vitro* hemotoxicity and *ex ovo* hemotoxicity of the nanoparticles.

The hazard potential was determined by distinguishing between hazard groups A–E (A = no risk, B = slight hazard, C = moderate hazard, D = serious hazard, E = severe hazard) according to ISO/TG 12901-2.

In the next step, the exposure score was calculated based on descriptions of the work of employees (ESI, Table 7†) in defined scenarios (Table 3), comprising:

  • working tasks, duration and frequency,
  • material and product characterisation,
  • cleaning, inspection, and maintenance (quality assurance) of the work place,
  • working environment, room size and ventilation, and
  • implemented control and risk management measures.

The overall nano-specific risk in occupational safety (1 = low, 2 = middle, 3 = high) was finally evaluated based on the exposure score and hazard group.

Results

(Co)LAVA technology as a promising new approach for the industrial manufacturing of high-quality spherical, oxidic nanoparticles, including crystalline, less-agglomerated ferromagnetic maghemite (γ-Fe$_2$O$_3$) and superparamagnetic γ-Fe$_2$O$_3$/amorphous SiO$_2$ core/shell (SiliFe) nanoparticles, has been investigated regarding potential future environmental impacts, occupational safety during production and elemental purity of the final nanoenabled product. The results were critically compared with two references: (i) wet chemical synthesis of Gadovist® as a product alternative in the envisaged field of application and (ii) FSP of oxidic nanoparticles as a process alternative.

Physicochemical characterisation

The physicochemical properties of crystalline γ-Fe$_2$O$_3$[24] and SiliFe nanoparticles,[23] produced *via* LAVA and CoLAVA methods, respectively, are summarised in Table 4 (further information, *e.g.* stability under storage, zeta potential, aging and degradation behaviour under physiological conditions, have been recently published by Rabel and colleagues[49]).

Table 4 Physicochemical characterisation of γ-Fe$_2$O$_3$[24] and SiliFe composite nanoparticles

Physicochemical properties	γ-Fe$_2$O$_3$	SiliFe
Mean particle diameter [nm]	23.2 ± 0.4	17.2 ± 0.1
Width of particle size distribution [nm]	33.1	18.7
Mean size of maghemite inclusions [nm]	—	11.0 ± 0.7
Mean crystallite size of maghemite [nm]	26.5 ± 0.2	5.9 ± 0.2
Specific surface [m^2 g^{-1}]	35.6	86.4
Saturation magnetization M_S [Am^2 kg^{-1}]	72.2 ± 2.2	11.6 ± 0.5
Relative remanence M_R/M_S	0.26	0.01

γ-Fe$_2$O$_3$ nanoparticles have a Fe$_2$O$_3$ content of 99.69%, an average particle size of 23.2 nm and a narrow size distribution and show a high saturation magnetisation of 72 Am^2 kg^{-1}. A relative remanence of 0.26 indicated ferromagnetic properties. The SiliFe composite nanoparticles have a lower Fe$_2$O$_3$ content of 36.29% and an average particle size of 17.2 nm with an inclusion (γ-Fe$_2$O$_3$ core) size of 11 nm. In comparison with the maghemite nanoparticles the width of their size distribution, given as the difference of the characteristic diameters d_{90}–d_{10}, was found to be decreased from 33.1 nm to 18.7 nm and the saturation magnetisation reduced from 72 Am^2 kg^{-1} to 11 Am^2 kg^{-1} due to the amount of non-magnetic silicon dioxide. Also, the relative remanence was reduced to 0.01 indicating superparamagnetic behaviour. The magnetic properties of IONs have a direct influence on the T_2 contrast and applications in MRI diagnostics, *e.g.* liver cancer therapy or islet cell transplantation.[19]

Based on the iron content, hypothetical mass doses of SiliFe and γ-Fe$_2$O$_3$ in a future diagnostic product were calculated based on known doses of the former contrast agents Feridex® and Resovist® (Table 2). SiliFe has to be applied in higher mass doses (231 mg and 154 mg per dose, respectively), due to the lower iron content, while mass doses of 84 mg and 59 mg per dose, respectively, were calculated for γ-Fe$_2$O$_3$ nanoparticles with an organic shell.

XRF measurements of the γ-Fe$_2$O$_3$ and SiliFe nanopowders regarding impurities of nickel, potassium, manganese, sulphur and zinc (ESI, Table 1†) per FU revealed that γ-Fe$_2$O$_3$ nanoparticles would fulfil the limits of elemental impurities for human use (Table 5), but in the case of SiliFe nanoparticles, nickel impurities (originating from the current silicon dioxide source) may lie above the threshold defined in the ICH-Q3D guideline[26] in case a high dose of 231 mg is needed in order to obtain a sufficient T_2 contrast.

Table 5 Elemental impurities of SiliFe and γ-Fe$_2$O$_3$ nanoparticles; compliance with maximum permitted daily exposure (PDE) for parenteral application per functional unit (FU) in accordance with ICH-Q3D

Nanoparticle	Mass dose (FU)	Elemental impurities in µg per FU		
		Ni (PDE = 22 µg)	Mn (PDE = 250 µg)	Zn (PDE = 1300 µg)
SiliFe	10 µmol Fe per kg bw	15 <PDE	92 <PDE	13 <PDE
γ-Fe$_2$O$_3$		6 <PDE	34 <PDE	5 <PDE
SiliFe	15 µmol Fe per kg bw	23 >PDE	139 <PDE	20 <PDE
γ-Fe$_2$O$_3$		8 <PDE	50 <PDE	7 <PDE

Life cycle assessment

Fig. 6 and 7 show exemplarily that the lower mass doses required in the case of γ-Fe$_2$O$_3$ nanoparticles have a distinct effect on all environmental impact categories (ESI, Fig. 2 and 3†) considered and would reduce the environmental impacts of the LAVA process compared to the CoLAVA process potentially by up to 60–65% (CoLAVA S2 and LAVA S6).

The comparison of the LCIA results between the wet chemical synthesis of the GCC Gadovist® taken as a reference (S1), and the (Co)LAVA production of the nanoenabled MRI agents shows a more differentiated picture. GWP (Fig. 6), EP (Fig. 7A), ADP$_{fossil}$, HTP and ETP (ESI, Fig. 2†) are increased in the case of the LAVA and CoLAVA processes (S2) whereas reductions in environmental impacts could be found in AP (Fig. 7B), ADP$_{elemental}$, ODP and POCP (ESI, Fig. 3†).

A hot-spot analysis of the alternatives, which shows the share of single process steps on the overall LCIA results, provided valuable insights. The hot-spot analysis of the CoLAVA process pointed out that the energy consumption of the carbon dioxide laser systems and the cooling unit dominates the LCIA results in all categories ($\geq$99%) (Fig. 8A), while during the synthesis of Gadovist®, the preparation of the educt butrol and related upstream processes seem to dominate most LCIA categories (Fig. 8B). The (Co)LAVA processes instead
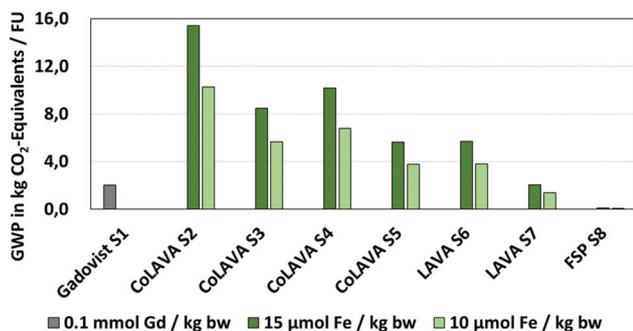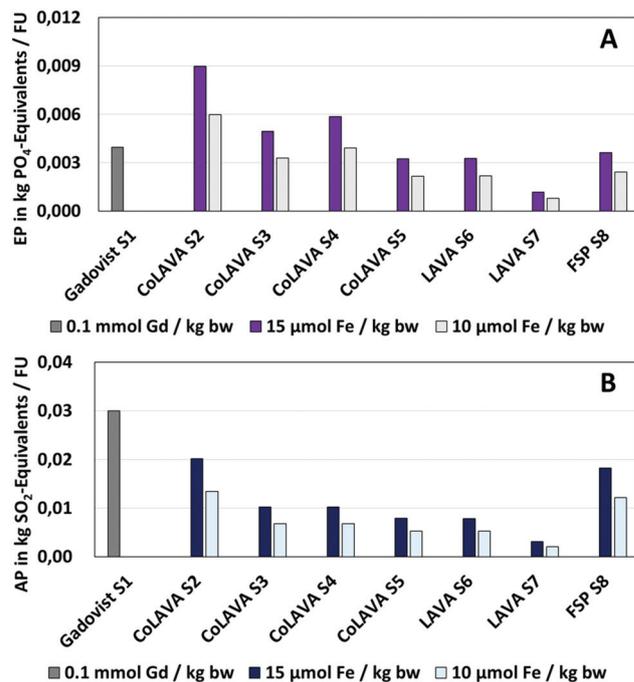

Fig. 7 LCIA of SiliFe nanoparticle synthesis by the CoLAVA process, γ-Fe$_2$O$_3$ nanoparticles by the LAVA process and FSP and as gadobutrol (Gadovist®) as a reference – acidification potential (A) and eutrophication potential (B).

require no metal catalysts or halogenated organic solvents, decreasing resource depletion and the environmental impacts and causing lower risks of halogen radical formation and ozone depletion reactions in the atmosphere.

Scenarios CoLAVA S3–S5 were analysed in order to identify strategies to reduce the high process energy demand of the laser vaporisation and cooling system, which dominates the LCIA outcomes (Fig. 6). Two promising strategies for a significant optimisation of the current LAVA process setup (installed at FSU on a laboratory scale) were identified, which can be easily implemented in the case of an industrial environment. The reuse of waste heat by the installation of a heating pump at the cooling unit, previously demonstrated in laser cutting processes,[39] would decrease the energy consumption in the CoLAVA process and the corresponding overall GWP by 45% (CoLAVA S3). An update of the laser source, *e.g.* using fiber or disk laser systems,[40] could reduce the energy demand of the laser system by 50% and the overall GWP by 33% (CoLAVA S4). Combining both, a decrease of the GWP up to 64% can be expected (CoLAVA S5).

The same optimisation strategy can be applied in the case of the LAVA process (LAVA S7). In combination with the benefits of a lower mass dose for one patient in the case of LAVA (Table 2) instead of CoLAVA generated oxidic nanoparticles, a more environmentally benign product than the GCC reference can be obtained in all LCIA categories considered, with the exception of the GWP, where similar values were obtained in the case of a mass dose of 15 µmol Fe per kg

Fig. 6 LCIA of SiliFe nanoparticle synthesis by the CoLAVA process, γ-Fe$_2$O$_3$ nanoparticles by the LAVA process and FSP and gadobutrol (Gadovist®) as a reference – global warming potential.
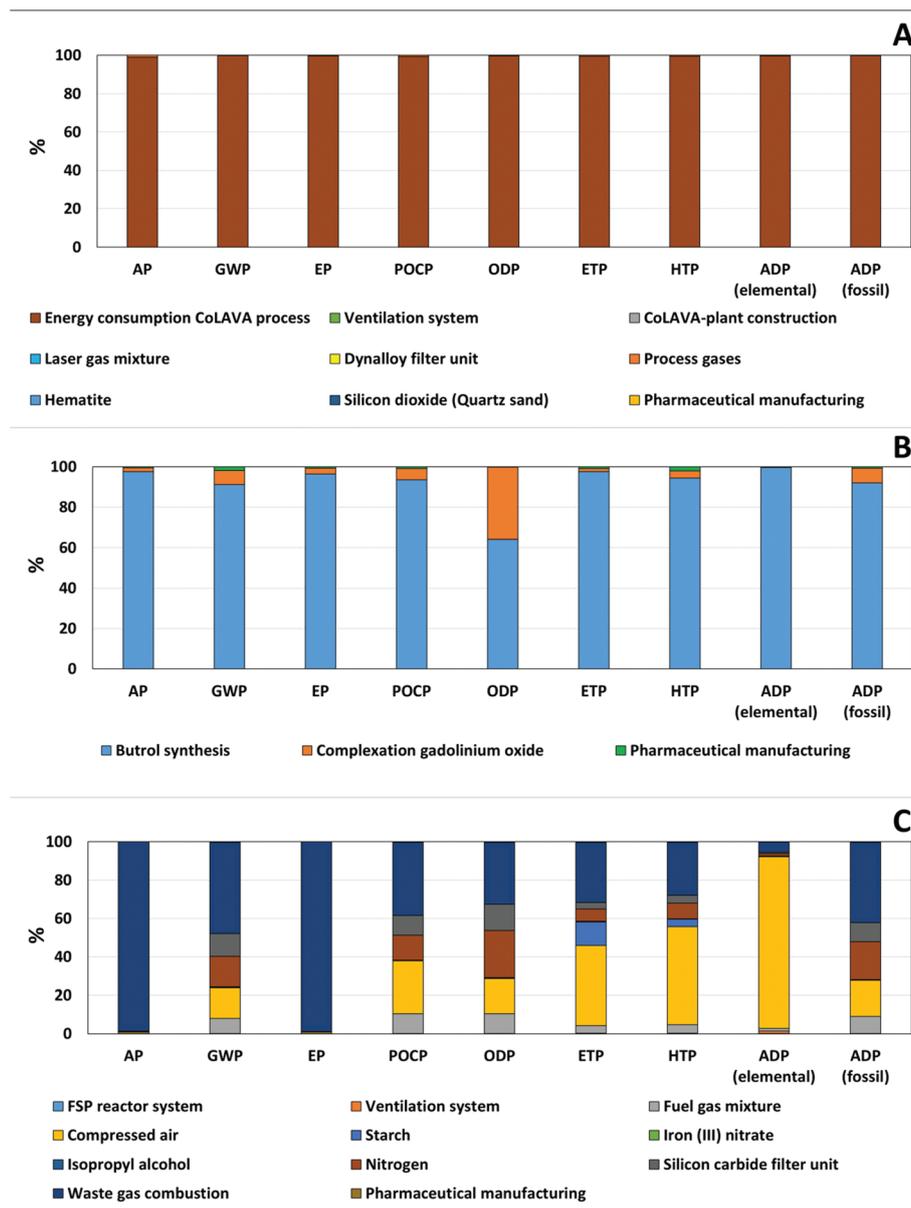
Fig. 8 Hot-spot analysis of environmental impacts of the synthesis of SiliFe nanoparticles by the CoLAVA process (A), gadobutrol (Gadovist®) (B) and γ-Fe$_2$O$_3$ nanoparticles by flame spray pyrolysis (FSP) (C). (AP = acidification potential, GWP = global warming potential, EP = eutrophication potential, POCP = photochemical ozone creation potential, ODP = ozone depletion potential, ETP = ecotoxicity potential, HTP = human toxicity potential, ADP = abiotic resource depletion).

bw (Gadovist S1: 2.03/LAVA S7: 2.06 kg CO$_2$ equivalents) (Fig. 6). The benefit in other LCIA categories ranges from 70–80% in the case of EP (Fig. 7A) to 90–94% in the case of AP (Fig. 7B) and POCP (ESI, Fig. 3†).

Finally, FSP was analysed as an alternative technology for oxidic nanoparticle generation *via* a gas phase synthesis (FSP S8). The hot-spot analysis revealed again the most critical process units in the overall synthesis process. In the case of FSP, the consumption of fuel and process gases for incineration and the need for cooling of the nanoparticles have the highest effect on the potential environmental impacts (≥84%

in all categories) (Fig. 8C). The consumption of nitrogen and the downstream waste gas combustion result in increased EP (Fig. 7A) and AP (Fig. 7B) by 309% and 599%, respectively, compared to LAVA S7, while other impacts were lower (*e.g.* reduction by 96% in the GWP (Fig. 6), 88% in the HTP (ESI, Fig. 2†) and POCP (ESI, Fig. 3†)).

Occupational safety analysis

Process schemes (ESI, Fig. 4†) were used for the identification of potential occupational risks in the design of alternative processes. In the LAVA and CoLAVA processes (ESI, Fig. 4†), the

preservation of homogeneity during the transport processes of the raw powder is a crucial step. The quality of the raw materials had to be checked and the homogeneity of raw powder mixtures in the CoLAVA process had to be ensured until the mixture reaches the vaporisation chamber. Safety precautions along the process especially in the context of laser light application, emissions of nanoparticles as aerosol and the emission of process gases are required. In FSP, the direct flame as well as the dosing of fuel and process gases and combustion of waste gases have to be operated in a controlled manner. In addition, safety requirements for the storage of inflammable organic solvents for precursor solutions have to be taken into account (ESI, Fig. 4†). In the case of Gadovist®, the safety requirements during storage, handling and treatment of chemicals and solvents are most important (ESI, Fig. 4†).

An occupational safety analysis on nano-specific risks was performed applying the control banding approach of Stoffenmanager Nano.[43] Since the investigation of the biological–toxicological effects of SiliFe and γ-Fe$_2$O$_3$ nanoparticles was still ongoing, the literature data were used for the identification of the hazard potential of a (theoretical) manufacturing process of the nanoenabled medical product. In ISO/TG 12901-2 different approaches are described, which can be used in the case of limited or missing specific hazard data by e.g. using a set of screening methods for biological–toxicological characterisation, by using the data of the bulk substance or by considering an analogous material instead.

Stötzel et al.[23] demonstrated similar surface properties of SiO$_2$ and SiliFe nanoparticles by comparative pH-dependent ζ-potential measurements on SiO$_2$, γ-Fe$_2$O$_3$ and SiliFe nanoparticles. Therefore, a closed SiO$_2$ surface of the SiliFe nanoparticles can be assumed. This finding was supported by high-resolution TEM micrographs of the SiliFe nanoparticles (Fig. 1). Therefore, selected hazard data of silicon dioxide nanoparticles[48] were evaluated regarding acute toxicity, skin and eye irritation, mutagenicity, cancerogenity and reproductive toxicity (ESI, Table 6†). The results were below the limits in the corresponding hazard group. Hence, hazard group A was assigned to silicon dioxide nanoparticles, and by that to SiliFe nanoparticles with a closed outer silicon dioxide shell (Table 6).

A post-process modification with starch was considered in hazard characterisation of γ-Fe$_2$O$_3$ nanoparticles, since the design of core–shell structures is a known strategy to ensure biocompatibility of IONs. Schlenk et al.[41] showed the relevance of the coating material for the assessment of the nanotoxicity of the coated iron oxide nanoparticles and pointed out that the coating with neutral organic polymers (e.g. starch) results in low toxic effects. Based on the results of this study, γ-Fe$_2$O$_3$ nanoparticles coated with starch were allocated to hazard group A (Table 6).

In the assessment of potential exposure, scenarios were defined (Table 6) covering the main stages in the processing of a contrast agent (based on the current installations and experiences with the (Co)LAVA and FSP setups) up to the final medical product (based on process schemes (ESI, Fig. 4†)). In Scenario A, a confined production plant and a continuous gas phase synthesis ((Co)LAVA or FSP) were assumed, monitored by engineers in a separate control room. Low exposure potential can be expected, since there is no direct contact with the produced nanoparticles (Table 6). Average exposure potential was obtained in Scenario B, considering the manual maintenance of the process plant. The exposure risk is increased due to the direct contact with agglomerated or aggregated nanoparticle residues in the breathing zone (<1 m) of employees. A consideration of different PPE (filter mask or full-face powered air respirator) did not alter the outcome. Scenario C takes into account the formulation and packaging step, comprising a sterile filling of the nanoparticles into an aqueous medium and the packaging of the final medical product. A low exposure risk was determined for this process step. During storage and transport (Scenario D), the exposure potential remained low, since there is again no direct contact of employees with the nanomaterials.

Overall, the potential nano-specific risks of SiliFe and γ-Fe$_2$O$_3$ nanoparticles were found to be low (Table 6). A confined process plant and standard safety measures during manufacturing, formulation and packaging (filter masks, ventilation) seemed sufficient to ensure occupational safety. Only working tasks requiring a direct contact with the nanopowder (or residues) should be given high attention and adequate control.

Discussion

Potential environmental impacts, elemental purity and occupational safety of spherical, oxidic nanoparticles produced by

Table 6 Occupational risk assessment of γ-Fe$_2$O$_3$ and SiliFe nanoparticles. Hazard potential was determined by distinguishing between hazard groups A−E (A = no risk, B = slight hazard, C = moderate hazard, D = serious hazard, E = severe hazard) according to ISO/TG 12901-2 (PPE = personal protective equipment)

Scenario		Comment	Hazard group		Exposure potential	Risk score
			γ-Fe$_2$O$_3$	SiliFe		
A	Production process for nanoparticles	(Co)LAVA or FSP	A	A	Low	Low
B	Maintenance of the process plant	No risk reduction by different PPE[a]	A	A	Average	Low
C	Manufacturing process of the final product	No separate filling system, use of different PPE	A	A	Low	Low
		Separate filling system, glove box and use of different PPE	A	A	Low	Low
D	Transport of the packaged product		A	A	Low	Low

[a] Personal protective equipment.

CoLAVA or LAVA were investigated at an early stage of process design in order to provide essential information and insights before a decision is made, whether the technology is suited for an efficient, environmentally benign and safe industrial production of nanoparticles for medical and pharmaceutical purposes.

The physicochemical characterisation (Table 4) of the magnetic nanoparticles confirmed the material properties required for the application of the nanoparticles as a T_2 contrast agent in MRI diagnostics.[19] Ferromagnetic nanoparticles such as γ-Fe_2O_3 characterised by a particle size above 20 nm are under investigation for highly sensitive MRI diagnostics, *e.g.* in the case of pancreas transplantation during the treatment of *diabetes mellitus*,[50] whereas superparamagnetic nanoparticles characterised by iron oxide domains with sizes between 4–20 nm such as SiliFe have been suggested for MRI diagnostics of liver carcinoma.[51] Thus, both types are in general suited for the envisaged application.

Based on the literature data, the toxicological and biological hazard potential of both SiliFe and γ-Fe_2O_3 nanoparticles has been classified as low, as long as the shell remains intact (Table 6). More detailed toxicological investigations (including *in vitro* hemocompatibility and cytotoxicity and *in vivo* long-term effects in mice) are ongoing and will be considered from the next step of the decision process, but the comparability with biocompatible materials described in the literature suggests a high likeliness of biocompatibility of the new products as well. Also the requirements concerning the elemental purity of pharmaceutical products[26] can be fulfilled by both nanomaterials (Table 5).

The results of the LCIA pointed out that at the current level of technological readiness, the high energy demand of the laser system may cause comparably high environmental impacts, if transferred to the industrial scale without further process optimisation (Fig. 6 and 8A). However, several process optimisation measures could be easily applied, resulting in a reduction of environmental impact potential such as the GWP of up to 64% (Fig. 6). Due to the higher benefit (magnetic properties) per potential environmental impact ratio, γ-Fe_2O_3 nanoparticles produced by LAVA and *post*-process coated with an organic shell have been found to be more promising for the envisaged application than core–shell SiliFe nanoparticles directly produced by CoLAVA. In the case of γ-Fe_2O_3 nanoparticles produced by LAVA, an optimised industrial production setup could potentially save significant environmental impacts per FU in all impact categories considered in the evaluation, when compared to the reference wet chemical synthesis of Gadovist®.

Comparing LAVA and FSP production of the same type of oxidic nanoparticle and after *post*-process organic coating gives a more balanced result. One benefit of FSP compared to LAVA is the lower energy demand[20] and the corresponding GWP at a comparable production rate. In contrast, the use of solvents and fuel gases causes extra emissions in the case of FSP, which do not occur in the case of LAVA, and results in higher AP and EP. Both technologies are likely further optimised during scale-up and industrial implementation and should be compared again at a later stage in order to potentially solve the current indifference of the LCIA results.

In terms of occupational safety, the requirements for both process alternatives are similar. There are comparable process specific risks in laser light (Co)LAVA or of open flames (FSP) resulting in comparable safety precautions (ESI, Fig. 4†). In comparison with the synthesis of Gadovist®, occupational safety requirements for the handling of chemicals seem to be lower for both gas phase synthetic routes, since no or less (isopropanol in the case of FSP) solvents or harmful educts are used. The multi-step Gadovist® synthesis instead requires heavy metal catalysts and harmful organic solvents, *e.g.* DMF and toluene in the upstream chemical manufacturing (Fig. 6).

Nano-specific risks, evaluated for (Co)LAVA and FSP, were classified as low, if the system is confined (Table 6), as *e.g.* described by Wegner *et al.*[35]

Wegner[35] furthermore reported low FSP production costs of less than 100 EUR kg^{-1} for simple oxides with raw materials being the highest cost factor. Although a comparative life cycle costing analysis still has to be performed, the difference in the market price of more than 75% in the case of the commercial preparations Endorem® and Gadovist® clearly suggests that oxidic nanoparticles can be competitively viable in medical applications such as contrast agents in MRI.

Conclusion and outlook

Although the production of nanomaterials at the industrial scale is still not common, a growing number of products are making use of the specific material properties of nanoparticles.[3] Among the most mature gas-phase synthesis techniques for the industrial manufacturing of oxidic nanoparticles are (Co)LAVA and FSP. They allow a controlled production of spherical nanoparticles of high purity and with narrow size distribution, a prerequisite for medical and pharmaceutical applications.

By means of this study we could show that a holistic environmental impact and safety assessment of new nanotechnologies such as Co(LAVA) and FSP, which are under continuous development and optimisation, is possible and provides helpful insights for informed decision-making prior to further scale-up and industrial implementation. The comparative study points out hot-spots for further efficient improvement of the process and the products alike, but confirms already the future potential for environmental savings in the case of industrial production of a nanoenabled diagnostic product compared to the state of the art. Furthermore, it gives substantiation to the assumption that occupational safety requirements during production can be met. The resulting products containing SiliFe or γ-Fe_2O_3 are suited for an application as T_2 contrast agents in MRI diagnostics and can fulfil elemental purity requirements according to the ICH-Q3D guideline.
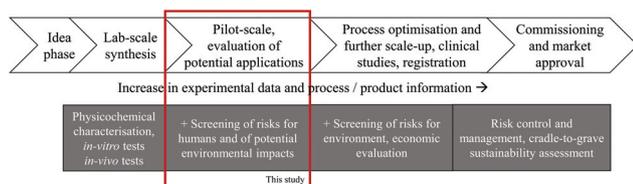
Fig. 9 Overall safe and sustainable innovation approach and placement of this study.

The work presented here is part of the German collaborative project NanoBEL. The NanoBEL evaluation concept follows a safe by design approach for the selection of different iron oxide nanoparticles (modified with a variety of organic and in-organic coatings) for future applications in diagnostics. The characterisation of physicochemical properties and biological–toxicological effects are complemented by qualitative RA and quantitative LCA along the overall nanoparticle life cycle. Multi-criteria decision analysis helps to point out critical parameters and best-suited and most benign formulations early in the development of novel, nanoenabled products.

A profound and comparative biological–toxicological characterisation of diagnostic nanoparticles produced by (Co) LAVA compared to wet chemical synthesis procedures is part of the ongoing study and will allow an advanced human health risk assessment during the next stage of the decision-making process. However, in order to obtain the full picture concerning the safety and sustainability of nanoenabled products, further studies focussing not only on humans but also on environmental risks (*e.g.* bioaccumulation and ecotoxicity) need to be performed. Among others, the collaborative European project BIORIMA investigates the environmental risks of nanomaterials depending on entry paths into the environment and further fate in the environmental compartments of air, water and soil. Taking all this increasingly available information together (Fig. 9), safe and sustainable nanotechnological innovations based on informed decisions could become a standard in the future.

Conflicts of interest

The authors confirm that no conflict of interest exists.

Acknowledgements

References

1 M. P. Tsang, E. Kikuchi-Uehara, G. W. Sonnemann, C. Aymonier and M. Hirao, *Nat. Nanotechnol.*, 2017, **12**, 734–739.
2 Z. Sun, T. Liao and L. Kou, *Sci. China Mater.*, 2016, **60**, 1–24.
3 Y. Wang and B. Nowack, *Environ. Pollut.*, 2018, **235**, 589–601.
4 W. J. Stark, P. R. Stoessel, W. Wohlleben and A. Hafner, *Chem. Soc. Rev.*, 2015, **44**, 5793–5805.
5 A. Oke, C. Aigbavboa and K. Semenya, *JAER*, 2017, **102**, 364–369.
6 A. C. Anselmo and S. Mitragotri, *Bioeng. Transl. Med.*, 2016, **1**, 10–29.
7 M. E. Vance, T. Kuiken, E. P. Vejerano, S. P. McGinnis, M. F. Hochella Jr., D. Rejeski and M. S. Hull, *Beilstein J. Nanotechnol.*, 2015, **6**, 1769–1780.
8 K. Cooper, *Micromachines*, 2017, **8**, 1–8.
9 A. D. Maynard, R. J. Aitken, T. Butz, V. Colvin, K. Donaldson, G. Oberdorster, M. A. Philbert, J. Ryan, A. Seaton, V. Stone, S. S. Tinkle, L. Tran, N. J. Walker and D. B. Warheit, *Nature*, 2006, **444**, 267–269.
10 SPIRE Roadmap, https://www.spire2030.eu/what/walking-the-spire-roadmap/spire-Roadmap (accessed May 2019).
11 C. Noorlander and A. Sips, *NANoREG Safe-by-Design (SbD) Concept*, RIVM and TEMAS AG, 2016.
12 D. Kralisch, D. Ott, A. A. Lapkin, P. Yaseneva, W. De Soete, M. Jones, N. Minkov and M. Finkbeiner, *J. Cleaner Prod.*, 2018, **172**, 2374–2388.
13 D. Kralisch, C. Staffel, D. Ott, S. Bensaid, G. Saracco, P. Bellantoni and P. Loeb, *Green Chem.*, 2013, **15**, 463–477.
14 D. Hou, S. Qi, B. Zhao, M. Rigby and D. O'Connor, *J. Cleaner Prod.*, 2017, **162**, 1157–1168.
15 Background document "Towards sustainability in SPIRE innovation projects", https://www.spire2030.eu/measure (accessed May 2019).
16 H.-D. Kurland, J. Grabow and F. A. Müller, *J. Eur. Ceram. Soc.*, 2011, **31**, 2559–2568.
17 A. Gutsch, M. Krämer, G. Michael, H. Mühlenweg, M. Pridöhl and G. Zimmermann, *KONA Powder Part. J.*, 2002, **20**, 24–37.
18 M. Wu, L. Gu, Q. Gong, J. Sun, Y. Ma, H. Wu, Y. Wang, G. Guo, X. Li and H. Zhu, *Nanomedicine*, 2017, **12**, 555–570.
19 H. J. Kwon, K. Shin, M. Soh, H. Chang, J. Kim, J. Lee, G. Ko, B. H. Kim, D. Kim and T. Hyeon, *Adv. Mater.*, 2018, e1704290.
20 S. Li, Y. Ren, P. Biswas and S. D. Tse, *Prog. Energy Combust. Sci.*, 2016, **55**, 1–59.

21 J. G. Penfield and R. F. Reilly, *Nat. Clin. Pract. Nephrol.*, 2007, **3**, 654–668.

22 A. K. Nehra, R. J. McDonald, A. M. Bluhm, T. M. Gunderson, D. L. Murray, P. J. Jannetto, D. F. Kallmes, L. J. Eckel and J. S. McDonald, *Radiology*, 2018, **288**, 416–423.

23 C. Stötzel, H. D. Kurland, J. Grabow and F. A. Muller, *Nanoscale*, 2015, **7**, 7734–7744.

24 C. Stötzel, H.-D. Kurland, J. Grabow, S. Dutz, E. Müller, M. Sierka and F. A. Müller, *Cryst. Growth Des.*, 2013, **13**, 4868–4876.

25 A. Erlebach, H. D. Kurland, J. Grabow, F. A. Muller and M. Sierka, *Nanoscale*, 2015, **7**, 2960–2969.

26 *ICH Guideline Q3D on elemental impurities*, The International Council for Harmonisation ICH, 2016.

27 *Guidance manual towards the integration of risk assessment into life cycle assessment of nano-enabled applications. Series on the Safety of Manufactured Nanomaterials No. 57, ENV/JM/MONO(2015)30*, Organisation for Economic Cooperation and Development OECD, 2015.

28 T. F. Stocker, D. Qin, G.-K. Plattner, M. Tignor, S. K. Allen, J. Boschung, A. Nauels, Y. Xia, V. Bex and P. M. Midgley, *Climate Change 2013: The Physical Science Basis. Contribution of Working Group I to the Fifth Assessment Report of the Intergovernmental Panel on Climate Change*, 2013.

29 V. Bach and M. Finkbeiner, *Int. J. Life Cycle Assess.*, 2016, **22**, 387–397.

30 Y. Emara, A. Lehmann, M. W. Siegert and M. Finkbeiner, *Integr. Environ. Assess. Manage.*, 2019, **15**, 6–18.

31 M. Wu, L. Gu, Q. Gong, J. Sun, Y. Ma, H. Wu, Y. Wang, G. Guo, X. Li and H. Zhu, *Nanomedicine*, 2017, **12**, 555–570.

32 https://www.amikon-shop.de/trumpf-tlf-6000-turbo-co2-laser/roboter/a-6404/(accessed May 2019).

33 https://www.lasercomponents.com/de/produkt/znse-linsen-fuer-co2-laser/(accessed May 2019).

34 D. H. Barr, PhD thesis, Naval Postgraduate School, 1972.

35 K. Wegner, B. Schimmöller, B. Thiebaut, C. Fernandez and T. N. Rao, *KONA Powder Part. J.*, 2011, **29**, 251–265.

36 G. Doka, *Ecoinvent Report No. 13*, Swiss Centre for Life Cycle Inventories, St. Gallen, 2009, p. 40.

37 J. Platzek, P. Blaszkiewicz, H. Gries, P. Luger, G. Michl, A. Müller-Fahrnow, B. Radüchel and D. Sülzle, *Inorg. Chem.*, 1997, **36**, 6086–6093.

38 Umwelterklärung TEVA 2017, https://www.ratiopharm.de/assets/media/Teva_RWD/Unternehmen/Teva_in_Deutschland/Umwelt/Teva_Umwelterklaerung_2017.pdf (accessed May 2019).

39 https://iqma-energy.de/wp-content/uploads/Energieeffizienz_Praesentation_iQma-energy.pdf (accessed May 2019).

40 K. Kellens, G. C. Rodrigues, W. Dewulf and J. R. Duflou, *Phys. Procedia*, 2014, **56**, 854–864.

41 F. Schlenk, S. Werner, M. Rabel, F. Jacobs, C. Bergemann, J. H. Clement and D. Fischer, *Arch. Toxicol.*, 2017, **91**, 3271–3286.

42 D. Beloin-Saint-Pierre, D. A. Turner, B. Salieri, A. Haarman and R. Hischier, *Int. J. Life Cycle Assess.*, 2017, **23**, 191–196.

43 B. Van Duuren-Stuurman, S. R. Vink, K. J. M. Verbist, H. G. A. Heussen, D. H. Brouwer, D. E. D. Kroese, M. F. J. Van Niftrik, E. Tielemans and W. Fransman, *Ann. Occup. Hyg.*, 2012, **56**, 525–541.

44 WHO, *Human Health Risk Assessment Toolkit: Chemical Hazards*, World Health Organisation, 2010.

45 https://www.ich.org/products/guidelines/safety/article/safety-guidelines.html (accessed May 2019).

46 J. Pietschmann, *Industrielle Pulverbeschichtung: Grundlagen, Anwendungen, Verfahren*, Vieweg+Teubner Verlag, Wiesbaden, 2013.

47 L. Gomez, V. Sebastian, S. Irusta, A. Ibarra, M. Arruebo and J. Santamaria, *Lab Chip*, 2014, **14**, 325–332.

48 *SILICON DIOXIDE: SUMMARY OF THE DOSSIER Series on the Safety of Manufactured Nanomaterials No. 71, ENV/JM/MONO(2016)23*, Organisation for Economic Cooperation and Development OECD, 2016.

49 M. Rabel, P. Warncke, C. Grüttner, C. Bergemann, H.-D. Kurland, R. Müller, V. Dugandzic, J. Thamm, F. A. Müller, J. Popp, D. Cialla-May and D. Fischer, *Nanomedicine*, 2019, **14**, 1681–1706.

50 N. Lee, H. Kim, S. H. Choi, M. Park, D. Kim, H. C. Kim, Y. Choi, S. Lin, B. H. Kim, H. S. Jung, H. Kim, K. S. Park, W. K. Moon and T. Hyeon, *Proc. Natl. Acad. Sci. U. S. A.*, 2011, **108**, 2662–2667.

51 Y. W. Li, Z. G. Chen, J. C. Wang and Z. M. Zhang, *World J. Gastroenterol.*, 2015, **21**, 4334–4344.